

Progress Report  
to the  
6th J-PARC PAC Meeting

J-PARC E06 (TREK) Experiment  
**Measurement of T-violating Transverse Muon  
Polarization in  $K^+ \rightarrow \pi^0 \mu^+ \nu_\mu$  Decays**

E06 (TREK) Collaboration\*

October 8, 2008

---

\*Contact person : J. Imazato (jun.imazato@kek.jp)

# Contents

<b>1</b>	<b>Introduction</b>	<b>3</b>
<b>2</b>	<b>Funding efforts</b>	<b>3</b>
2.1	Efforts in Japan . . . . .	3
2.2	Funding for target R&D in Canada . . . . .	3
2.3	Funding efforts in the U.S.A. . . . .	4
<b>3</b>	<b>Detector R&amp;D and design status</b>	<b>4</b>
3.1	Muon polarimeter chamber and muon field magnet . . . . .	4
3.1.1	Concept of an the active polarimeter . . . . .	4
3.1.2	Current design . . . . .	5
3.1.3	GARFIELD calculation . . . . .	6
3.1.4	Prototype test with a 1/5-size model . . . . .	7
3.1.5	Schedule . . . . .	7
3.1.6	Muon field magnet . . . . .	8
3.2	Other detector elements . . . . .	9
3.2.1	Target fiber readout with MPPC . . . . .	9
3.2.2	Target fiber test with beam . . . . .	10
3.2.3	CsI(Tl) readout development . . . . .	10
3.2.4	Status of GEM development . . . . .	11
<b>4</b>	<b>Systematic error due to misalignments in the polarimeter</b>	<b>12</b>
4.1	Necessity of the study of local misalignments . . . . .	12
4.2	Possible misalignments and sources of systematic errors . . . . .	12
4.3	Left-right structural asymmetry in the staggered wire configuration . . . . .	13
4.4	Effects of wire misalignments . . . . .	14
4.4.1	Spurious asymmetry distribution and spurious polarization . . . . .	14
4.4.2	Several considerations . . . . .	15
4.4.3	Monte Carlo studies . . . . .	15
4.4.4	Discussions . . . . .	16
4.5	Effects of non-uniform chamber inefficiency . . . . .	17
<b>5</b>	<b>Summary</b>	<b>18</b>

# 1 Introduction

In this short note we will briefly report on our progress in preparations for the E06 (TREK) experiment since the last PAC meeting in June 2008. Although the period is only 4 months long and we have not very much to present, we regard it as our responsibility to update the PAC concerning our funding efforts and detector preparation status, since the PAC's view for the TREK approval status is that "*more progress will be needed on this front (of funding) before a stage-2 approval recommendation can be granted*" as was clearly stated in the minutes of the last meeting. We appreciate the appropriate detailed evaluation of our detector R&D and Monte Carlo simulation activities by the PAC. The understanding of the systematics in this high precision TREK experiment is crucial to the success of the experiment and such studies will not be complete until the end of the experiment. Needless to say the analyses of the systematic errors are particularly important in the detector design phase to feedback the results to the design. Currently we are designing the muon polarimeter chamber and magnet. A prototype drift chamber has been constructed and this is now being tested. We will present a consideration on the systematic errors associated with the drift chamber construction, which is a so-called error due to "local misalignment" and which has not yet been taken into account in the polarimeter global misalignment studies reported before. We will also present some other R&D and test experiment activities which are being carried out or planned for the very near future.

## 2 Funding efforts

### 2.1 Efforts in Japan

The only possibility to obtain so-called "external funding" for particle and nuclear physics projects in Japan is to apply for Grant-in-Aid research support. In the last meeting we reported that we were funded for part of the muon polarimeter construction in the category of "Basic research (A)". Twelve sets of drift chambers and a set of muon magnet are being designed and will be constructed during the three JFY period of 2008-2010. Unfortunately, the application to the newly established category "New Science Field" which would have covered the remainder of the detector construction and execution of the experiment for 5 years was not successful. This year we will continue the efforts to obtain additional Grant-in-Aid research support money. The current application rules of the Grant-in-Aid money system set rather strange constraints on the possible categories for a running project with a certain category in hand. We will be able to apply for the category of "Specially promoted research" which provides, if successful, a large amount of money which will be sufficient to complete the TREK detector and operate the experiment. We will request about 350 Myen for 5 years starting in JFY2009 with the main cash-flow for detector construction in 2009-2011.

### 2.2 Funding for target R&D in Canada

The contribution from the Canadian group to the K1.1-BR beamline construction has been the basic plan of the international cooperation in the TREK experiment. Toward this end an effort is being made in Canada. In July Prof. M. Hasinoff (University of British Columbia) prepared a grant request for C\$750K to the Canada Foundation for Innovation

(CFI) for funds to construct 2 quadupole magnets and one dipole magnet for the K1.1BR low momentum leg. Unfortunately, UBC has a maximum quota of 100M\$ and this grant was not considered to be important enough to any on campus UBC research program so it was not approved at the University level this year. There might be a chance to resubmit the request if there is another CFI competition next year.

Prof. M. Hasinoff is now preparing an equipment request for the Natural Sciences and Engineering Research Council (NSERC) to supplement the 3 year project grant which began in April'08. This additional equipment grant would provide funds specifically for the new scintillating fibre target and readout system. The extra equipment funds would allow the existing operating funds (on which we reported in the last meeting) to be used for the salaries of a post-doctoral research associate and graduate students as well as essential travel, *etc.* The total amount of this new equipment request is 100K\$.

### **2.3 Funding efforts in the U.S.A.**

In September 2008 the Hampton University group led by Prof. Michael Kohl submitted a grant proposal to the US National Science Foundation (NSF) with the title: "OLYMPUS and TREK: Two Precision Experiments to Determine the Two-Photon Exchange Effect in Lepton-Proton Scattering and to Search for New Physics Beyond the Standard Model", with a total of about \$600k over three years. This proposal aims to provide Prof. Kohl with base funding for his research activities and to establish a new lab on the campus at Hampton University dedicated to develop and construct detectors for TREK and OLYMPUS based on GEM (Gas Electron Multiplier) technology. Funds have been requested to pay for students and one postdoc, and for travel. Prof. Kohl is planning to start this activity by building a simpler set of GEM detectors for the OLYMPUS experiment proposed at DESY, for which a request of \$115k in equipment funds has been included. With the OLYMPUS experience, the more complex requirements of the GEM detectors for TREK can be more reliably fulfilled. It is anticipated to separately apply for equipment funds for construction of the TREK tracking detectors, via the MRI (Major Research Instrumentation) program of NSF which has the next due date in January 2009. Such an attempt, however, according to information from NSF, can only be successful if a full approval and a confirmed schedule for TREK can be given, to minimize NSF's risks. We also express the expectation that some if not all of the pure equipment cost for the GEM detectors of TREK may eventually be covered by Japanese funds, provided that Prof. Kohl's group at Hampton University can provide the infrastructure and personnel resources to carry out development, construction and testing locally at Hampton University. The GEM lab at Hampton University will greatly benefit from the strong partnerships with Jefferson Lab and MIT.

## **3 Detector R&D and design status**

### **3.1 Muon polarimeter chamber and muon field magnet**

#### **3.1.1 Concept of an the active polarimeter**

The most essential component of the TREK detector is the muon polarimeter. The transverse muon polarization will be measured with high precision by suppressing the systematic errors. Since any systematics in the polarimeter can induce a spurious asymmetry of the

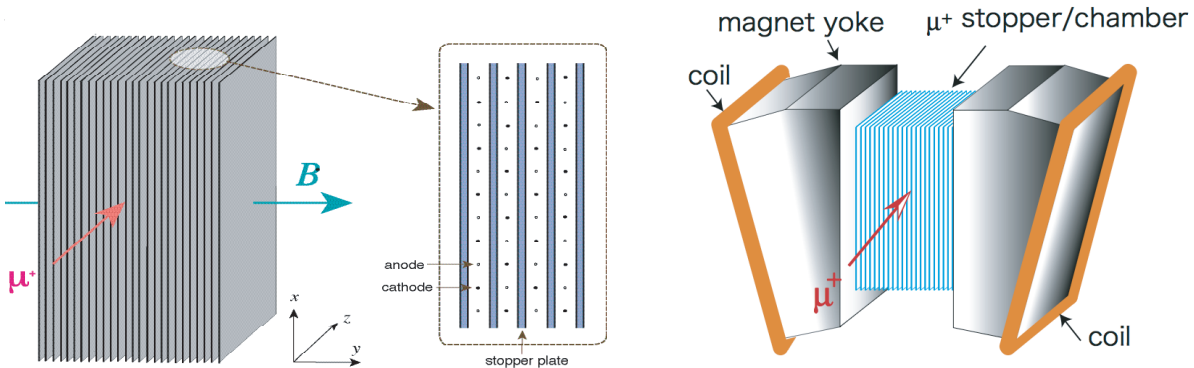


Figure 1: Schematic view of the active polarimeter with the drift chamber arrangement (left), and the configuration in the muon field magnet (right). The coils are in different positions in the most recent design.

decay positrons directly, careful design and manufacturing are required. The acceptance of the positron in the polarimeter is one of the decisive factors in determining the total acceptance of the detector, namely the sensitivity of the experiment. A background-free measurement in the polarimeter is one of the prerequisite conditions for this high precision experiment. By using the Grant-in-Aid research support budget provided for the polarimeter construction, the polarimeter is now leading the TREK detector upgrade.

In the current design of the polarimeter we put the highest priority on the forward and backward  $\pi^0$  scheme of the  $K_{\mu 3}$  kinematics, which we adopted in the previous E246 experiment and which we also regard to be the most reliable data with drastically suppressed systematic errors in the TREK experiment. The polarimeter is designed so as to measure primarily the azimuthal positron asymmetry (or left/right asymmetry in the gap local coordinate), although other asymmetry components corresponding to different  $\pi^0$  kinematics are also possible to analyze after a more elaborate systematics study.

### 3.1.2 Current design

The detector part of the polarimeter consists of several muon stopper plates with gaps in between, and drift chamber layers in these gaps. Fig.1 shows the conceptual configuration with the muon field magnet and Fig.2 shows the current design of the stopper and drift chamber cell structure. In the current design the wire coordinate redaout is done by means of charge division. The normal direction of the plates is the azimuthal direction along which we measure the left/right positron asymmetry, and the sense wires are strung in the radial direction. The cell structure of the chamber is chosen to have a rather large aspect ratio of 2.0 after elaborate GRAFIELD calculations by two independent groups in Japan and in Canada and taking into account the cost which can be reduced proportionally to the aspect ratio. Since the tracking performance is limited mainly by the scattering in the stopper plates (Fig.3), there is considerable room to compromise the chamber performance. Regarding the tracking resolution a series of Monte Carlo simulation calculations have been

Table 1: Main parameters of the muon polarimeter chamber

Parameter	Value
Size	284 mm (w), 700 mm (h), 320 mm (d)
Number of chamber layers	25
Stopper width as Al	2.5 mm
Gap	8.0 mm
Anode wire pitch	16.0 mm
Anode wire	to be determined in the prototype test
Gas	Ar+Ethane (50%+50%)
Wire coordinate readout	charge division (or cathode readout)
Effective number of analysis layers	4 ~ 5
Decay vertex resolution in $z$ ( $\sigma$ )	0.5 mm @ $0^\circ$ , 1.0 mm @ $67^\circ$ for 30 MeV $e^+$
Angular resolution in $z$ - $y$ ( $\sigma$ )	$\sim 10^\circ$ for 30 MeV $e^+$

performed. Table 1 summarizes the main parameters and performance of the chamber. Fig.3 illustrates typical positron trajectories.

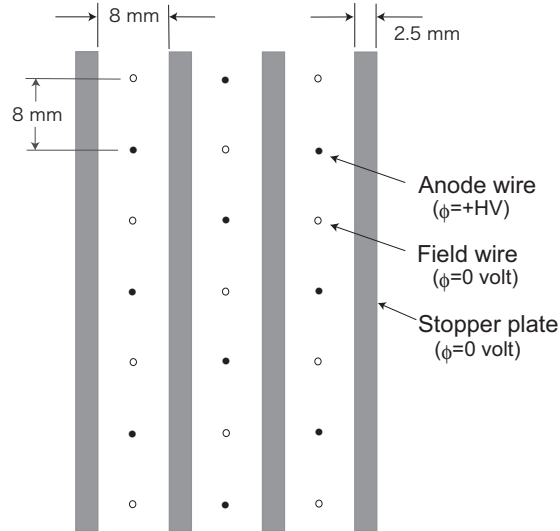


Figure 2: Cell structure of the gap drift chamber with a large aspect ratio of 2.0. There are several candidate materials for the stopper plates [1].

### 3.1.3 GARFIELD calculation

The main purpose of chamber cell electric field calculation with GARFIELD was to investigate the field distribution characteristics of the elongated cell, in order to check the anode wire signal for different charged particle tracks to determine the isochronous drift time and the timing resolution. Finally a drift time table was calculated as a function of the charged

particle penetrating coordinate and its angle in a cell in order to provide the calibration for the track reconstruction.

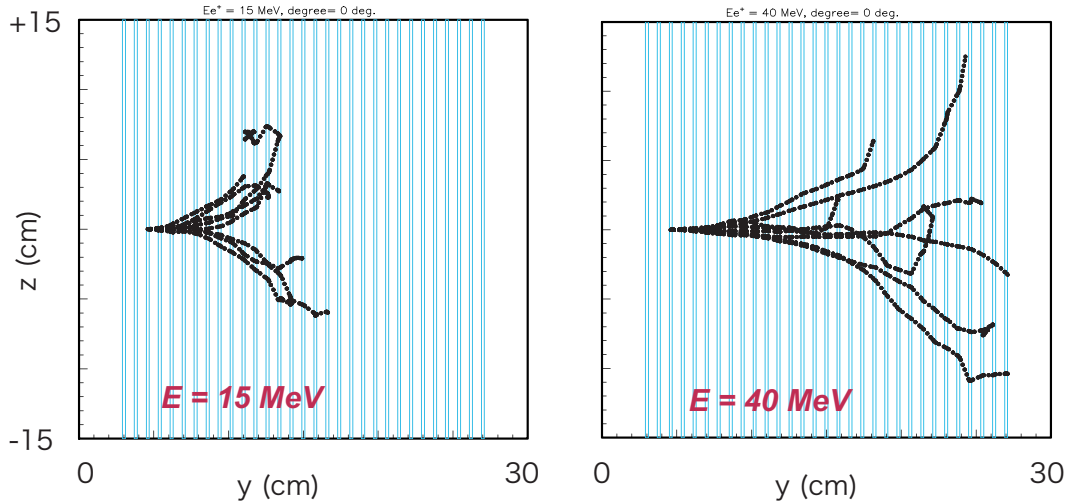


Figure 3: Typical positron trajectories in the MC simulation with scattering in the stopper plates for  $E_{e^+} = 15$  MeV (left) and 40 MeV (right). Initial emission angle is zero degree. Pure Al plates were assumed as the stopper in this calculation.

### 3.1.4 Prototype test with a 1/5-size model

In order to confirm the basic drift chamber function with the elongated cell and also to study the readout method for the  $r$ -direction (along the sense wires), a so-called 1/5 model has been constructed with only five drift layers. An important issue here is the study of the inefficiency distribution in the cell. There are two schemes which are conceivable to measure the  $r$ -coordinate while keeping the present stopper plate scheme: one is to adopt sense wire charge division and the other is the cathode readout technique by splitting the stopper plates (as cathodes) into strips. Although the latter certainly provides better position resolution, we are testing the former technique in the 1/5 model, because of its much lower cost and the adequacy of moderate position resolution in the present case. The latter requires a much more sophisticated positioning (or alignment) method of the split stoppers.

In the prototype several different types of anode wires of high resistance are strung to investigate their performance, especially the matching to the preamplifiers designed for this chamber using the chip designed by Dr.T.Taniguchi of the KEK electronics group. After confirming the basis performance with a beta-ray source, this prototype chamber will be tested using the electron beam at Fuji Test Beam Line (FTBL) at KEK in November.

### 3.1.5 Schedule

After we confirm the chamber performance with the 1/5 prototype model and decide on an  $r$ -coordinate readout method, we will proceed to a full-size chamber model for one gap, which should be applicable as one of the 12 real units if it has sufficiently good performance. This

model will be tested not only for the chamber performance but also for the performance of muon polarization measurement. This chamber will be constructed using the best stopper material [1] and with the high machining and assembly precision required for the final model. This chamber will be tested using a polarized muon beam at TRIUMF next year in conjunction with the muon field magnet described below. The preamplifier system will also be finalized by that time. In the test experiment the analyzing power will be measured and the absence of any spurious asymmetry sources will be confirmed.

### 3.1.6 Muon field magnet

As was reported in the last meeting, the field distribution, in particular, the global symmetry of the field distribution on the muon stopper is one of the major decisive factors of the experiment. A new magnet system will be made to produce an ideal field distribution on the stopper. We now plan to manufacture a one gap magnet to test its field performance and also to be combined with the full-size chamber model for the polarization investigation. Magnetic field calculations have been done using a 2D code as well as 3D code. The field shimming to produce a field distribution as flat as possible with a yoke of reduced weight has been studied. Fig.4 shows the current design of the one gap magnet test arrangement and Fig.5 is the flux distribution. A magnetic field strength of 0.03 T is generated over the region of the wire chamber.

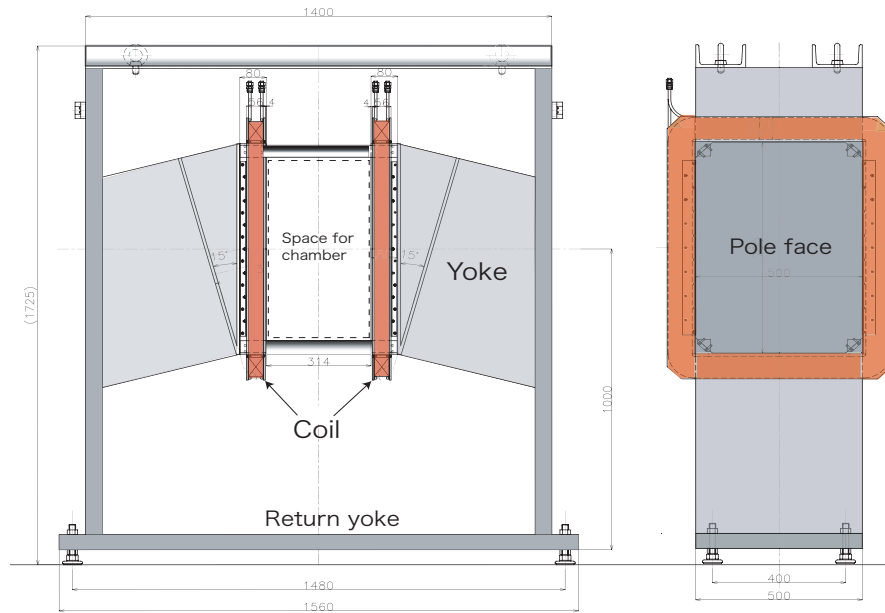


Figure 4: Schematic view of the muon field magnet in the one sector test arrangement

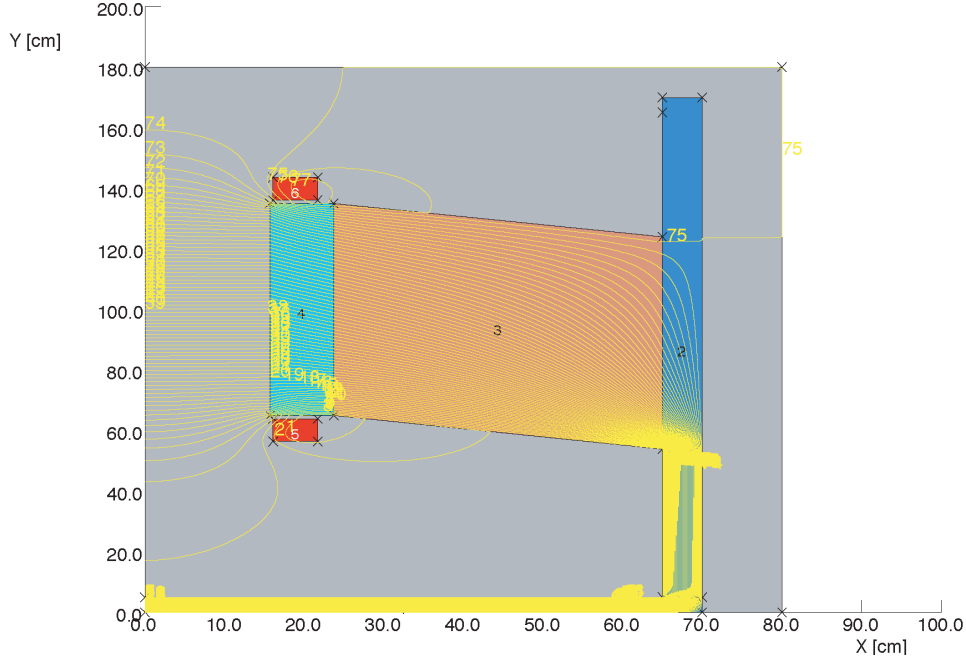


Figure 5: Magnetic flux density distribution in the muon magnet one sector test arrangement. Only the symmetric right region is shown with the median plane on the left boundary. If we adopt a low density iron return yoke (braun part), it can reduce the weight of the new magnetsystem.

## 3.2 Other detector elements

### 3.2.1 Target fiber readout with MPPC

The current design of the target fiber readout is to use an avalanche photo-diode with high internal gain in Geiger mode operation (MPPC) which is developing very quickly these days, as we described earlier in the proposal and the report to the FIFC. In the 3rd PAC meeting the radiation hardness of this device was questioned in view of the damage test result using a proton beam at RCNP. Although our backup plan from the beginning has always been the use of a multi-anode PMT, we want to pursue the adoption of MPPC since it has several advantages. Also the immunity to radiation is also being improved in recent products. In fact the result of the proton irradiation showed a rather crucial conclusion about the application of such MPPCs in the vicinity of beam axis. However, the relevant beam particles in TREK are pions and kaons. The MPPC damage by a pion beam is not well known although there is a scaling model in the “non ionization energy loss (NIEL)” theory from the proton beam damage; however its validity has not yet been confirmed experimentally. We will perform a pion beam irradiation test soon using a pion beam with high intensity at TRIUMF. The pion beam has a momentum of 140-150 MeV/c where the difference from the proton irradiation data might be expected to appear. The beam time is scheduled this month from Oct 18-24.

### 3.2.2 Target fiber test with beam

The new active kaon stopping target will be made with finer segmentation and with a smaller diameter than the E246 target. A bundle of 489 fibers with rectangular cross sections of 3 mm will be used to construct a new target of diameter 75mm. In order to match the requirements for a high precision experiment and also to construct a system which works in a high intensity beam environment, we plan to use the Wave Length Shifter (WLS) fiber for the readout of the light signal. The Canadian group is currently constructing several small 10 cm long scintillating fibres ( of area  $4 \times 4 \text{ mm}^2$  ) with 2 grooves ( 1mm wide ) cut into them ( similar to the FAST target at PSI ) in order to test the possibility of using flexible WLS fibres to readout the light into an MPPC or multi-anode PMT. Test pieces cut out from BC408 scintillator sheets as well as extruded scintillator manufactured for the BNL KOPIO experiment are being evaluated. We plan to test these first with sources and then in a 140 MeV/c pion/muon beam using the M13 and M11 pion channels at TRIUMF in the next few months. The overall light yield for each possible option will be measured.

### 3.2.3 CsI(Tl) readout development

The main part of the CsI(Tl) photon calorimeter upgrade is the substitution of the PIN photo-diode readout with a new faster APD+FADC system. The  $5 \times 5 \text{ mm}^2$  Hamamatsu S8664-55 avalanche photo-diodes are considered to be photo-detectors with well established and stable operation. The internal APD gain of 50-100 makes possible the use of fast amplifiers in order to increase the counting rate capability by  $\sim 10$  times compared to the previous PIN-diode readout. The simultaneous digitization of the CsI(Tl) signal by a flash-ADC will allow the rejection/reconstruction of pile-up events at rate of 300-500 kHz per single CsI(Tl) module. The performance of such a APD+FADC readout scheme together with the fast charge-sensitive amplifier was tested using a positron beam (100-400 MeV) at the Laboratory of Nuclear Science of Tohoku University last December. The reliability of the readout was proven with a high singles rate condition. Also, pileup events at the highest instantaneous beam rate were collected and analyzed to check the feasibility of their reconstruction. Pileup events were fitted to a superposition of two functions, where the shape of the function was evaluated from the non-pileup single events. It was also shown that the efficiency of two pulse separation is about 100% for a distance between the pulses greater than  $0.8 \mu\text{s}$ . The amplitude of the first pulse in the pileup event was reconstructed in an appropriate way. For the second pulse analysis, however, the situation is more complicated due to the presence of the overshoot and the ringing in the amplifier output. It was found that the reconstructed amplitudes for the second pulse have a rather broad distribution and, therefore, poor energy resolution. This result is explained by the fact that prototype charge sensitive amplifier has some differential/integration function which damaged the original unipolar APD signal. Obviously, the performance of the fast amplifier has to be improved. The ideal current amplifier would avoid the above mentioned drawbacks. A month ago a prototype of such a current amplifier was designed and assembled at INR (Moscow). At present, it has been tested with cosmic ray events using the same CsI(Tl)+APD system. One can expect a much better signal-to-noise ratio as well as an undamaged signal shape in the amplifier output. The modified readout should allow the efficient event reconstruction up to an average counting rate of 300-500 kHz.

### 3.2.4 Status of GEM development

The results from the test experiment with the MIT GEM telescope prototype conducted at Fermilab in 2007 have been submitted for publication [2]. We reported about this test experiment in the 4th PAC meeting in 2007 in detail.

The Hampton University Nuclear Physics group, of which Prof. Kohl is a member, has provided one graduate student of Hampton University (Ozgur Ates) since May 2008 to work with Prof. Kohl on a baseline design for the C0 and C1 detector elements. Over the summer of 2008, the student learned to use the GEANT4 simulation toolkit of CERN. The geometry of the TREK target along with the tracking detector elements C0, C1, and C2 residing in the field-free inner region of the TREK toroid was coded. An example output is given in Fig.6.

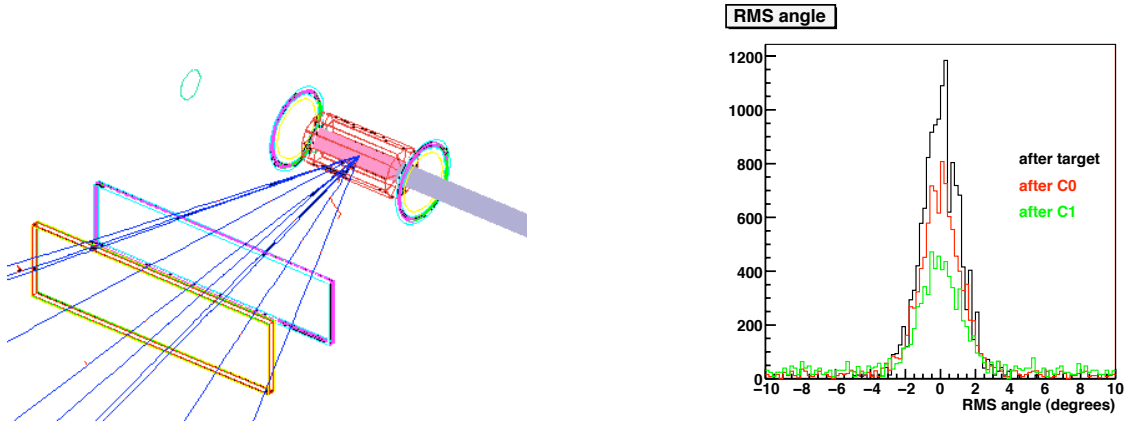


Figure 6: Left: GEANT4 view of TREK target and detector elements C0, C1 and C2. Right: Study of multiple scattering

Several goals of this approach are currently being pursued:

- Study of multiple scattering on muon tracks due to materials of the target and the GEM chambers C0 and C1
- Model realistic conditions including kaon stopping distribution and acceptance-defining apertures of CsI(Tl) calorimeter
- Study of the track reconstruction using straight tracks in C0, C1 and C2, with regards to vertex and angular resolution.
- Obtain design criteria for the dimensions of C0 and C1, density of readout channels, and the material budget.

The r.h.s. of Figure 6 shows the angular spread of 100 MeV muons originating from the target center, after exiting the target (black), after passing the C0 element (red), and the C1 element (green).

## 4 Systematic error due to misalignments in the polarimeter

### 4.1 Necessity of the study of local misalignments

The misalignments of the polarimeter and the muon field are the sources of the most dangerous systematic error since they induce a spurious asymmetry of the decay positrons directly. In particular, the misalignments or rotation as a unit (or in total) which we call "global misalignments" may admit the large in-plane polarization,  $P_N$  and  $P_L$  to the  $P_T$  component and they are serious. In the reports to the previous PAC meetings we have discussed this point, but we have also shown that there is a novel analysis method to extract  $P_T$  regardless of the existence of such misalignments. A high statistics Monte Carlo calculation could demonstrate the validity of this scheme.

It is quite natural that a question was raised about the effects of local misalignments in the polarimeter, namely the fine structure of the misalignments after the subtraction of the average (or global misalignments). In general, most kinds of local misalignments are averaged out resulting in an almost null effect depending on the nature, size and typical periodicity of the misalignment spatial variation. However, the necessity to check the influence of local misalignments in the polarimeter cannot be denied considering the decisive role of the polarimeter in this experiment. We are just now designing the polarimeter chamber and constructing a prototype. We have to have some criteria on the machining and assembly precision to specify to the manufacturer. Another question concerns the non-uniform chamber inefficiency which might also result in a local spurious asymmetry. We have been studying these problems since the last PAC meeting and we will present some results below.

### 4.2 Possible misalignments and sources of systematic errors

Nowadays all the components of the drift chamber and stopper plates are NC-machined and hence the accuracy of dimension is as high as 30 to 50  $\mu\text{m}$ . The sense wires and field wires are strung through plastics feed-throughs fixed in the holes NC-bored in the end-plates. Thus, positioning of the wires will be not much worse than several 10  $\mu\text{m}$ . However, the following misalignments are still conceivable. Here we regard the wire coordinate system as the reference system.

- (1) Random displacement of the wire positions due to the limited accuracy of soldering the wires to the feed-throughs and accumulated position inaccuracy of the feed-through.
- (2) Random displacements of each stopper position relative to the wire coordinate system.
- (3) Some systematic displacement of the stopper plates in total relative to the wire system.
- (4) Deformation of the chamber as the total structure.
- (5) Structural asymmetry due to the staggered wire configuration. This is not a misalignment but we put a consideration below.

In the data analysis we extract primarily the emission angle of the decay positrons relative to the wire coordinate system to deduce the asymmetry. The so-called "integral method" sets a cut on the angle. Thus the effects affecting the emission angle are essential. The

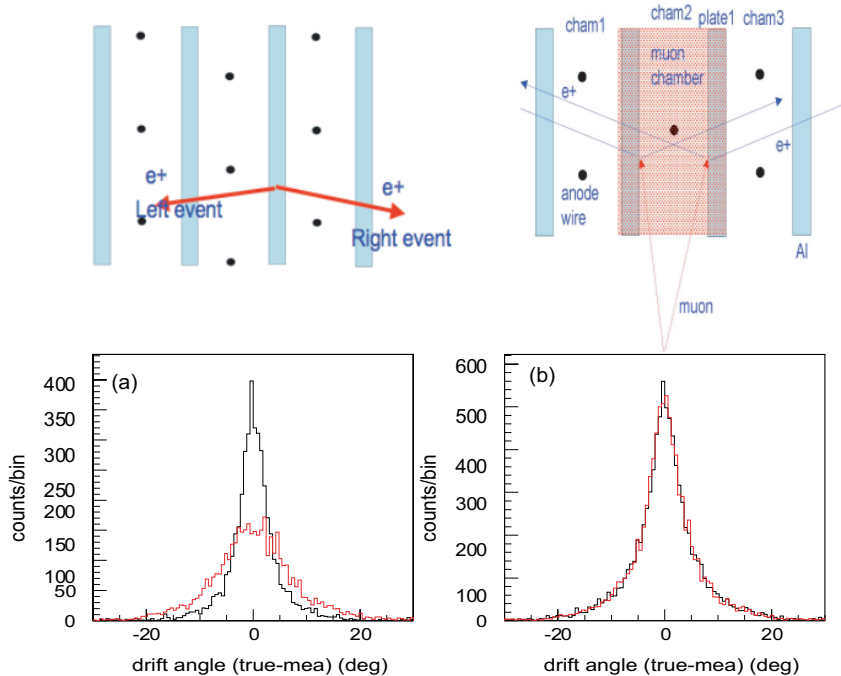


Figure 7: Analysis scheme with left/right asymmetry (left) and without asymmetry (right) for the staggered wire configuration. The angular response functions (the difference between the true emission angle and measured angle) are plotted. The black and red histograms are for the LHS and RHS, respectively.

ambiguity of the muon stopping points has only a secondary meaning unless we set a sharp cut on the stopping point. Therefore, items (2) and (3) should not have a large effect. Only three effects should be kept in mind for further discussions, although their sizes must be negligibly small. One is the scattering characteristics from a tilted plate which might slightly affect the average positron angle after the plate. The second is the influence on  $E_{e^+}$  determination which is done in terms of the number of penetrated stopper. The other is the inaccurate muon stopping distribution function determined experimentally which eventually becomes important in the final analysis. Item (4) is almost equivalent to the global misalignments and is not relevant now. The random displacement of the wires solely affects the measurement of the positron emission angle and has to be studied in detail.

### 4.3 Left-right structural asymmetry in the staggered wire configuration

The staggered configuration of the sense wires and field wires is the necessary requirement for reliable tracking with higher resolution. However the concern here is about the local

left/right structural asymmetry seen from a certain muon stopping point in a stopper plate. This might lead to a systematic error through the different left/right angular trace back characteristics. The lower part of Fig.7 shows the angular response function defined as the difference between the true emission angle and the fit emission angle at a certain muon stopping point near the anode wire. We observe fairly different resolution functions for left and right. Although this left/right asymmetry can be corrected for in the analysis and moreover, the effect is averaged out when we consider the whole chamber volume, a residual spurious asymmetry might be significant.

In order to overcome this concern, we will adopt the method of degenerate stopper plates at the cost of one layer of information. We do not care about which plate of the relevant chamber layer is the muon stopping plate as is illustrated in the upper part of Fig.7. Seen from the chamber gap, the left/ structural symmetry can be restored. The disadvantage here is the slight degradation of the tracking resolution due to the effective loss of one layer of data, but it is harmless in the view point of the systematic errors. With this scheme we can also avoid the inherent asymmetry due to the presence of an incident muon track and its signal.

## 4.4 Effects of wire misalignments

### 4.4.1 Spurious asymmetry distribution and spurious polarization

We will now consider the effects of anode wire misalignments. The primary consequence of the misalignments is the offset of the analyzed positron emission angle. In the integral analysis, where we set a cut on the emission cone angle from the azimuthal coordinate axis, the emission rate in this cone can be affected resulting in spurious asymmetry for muons stopping at a certain position in the stopper. Although such an asymmetry is fluctuating if we assume randomness in the wire displacement, and the final effect should be almost vanishing after the integration over the total stopper volume, we need to check the degree of cancellation. In order to simplify the discussion and concentrate on the analysis method which we regard most promising at the beginning, we assume the pion  *fwd+ bwd*  scheme. The spurious  $P_T$  due to local effects,  $\delta P_T^{sp}$  is expressed in general in terms of the spurious asymmetry distribution  $\delta A^{sp}(\vec{r})$  as

$$\delta P_T^{sp} = \int \delta \tilde{\rho}(\vec{r}) \cdot \frac{\delta A^{sp}(\vec{r})}{\alpha(\vec{r})} d\vec{r} \quad (1)$$

where  $\alpha$  is the analyzing power coefficient. The integration is taken over the entire stopper volume.  $\delta \tilde{\rho}(\vec{r})$  is the difference of the normalized muon stopping distribution for  *fwd*  events and  *bwd*  events, namely

$$\delta \tilde{\rho}(\vec{r}) = \tilde{\rho}_f(\vec{r}) - \tilde{\rho}_b(\vec{r}) \quad (2)$$

with

$$\tilde{\rho}_f(\vec{r}) = \rho_f(\vec{r}) / \int \rho_f(\vec{r}) d\vec{r} \quad (3)$$

$$\tilde{\rho}_b(\vec{r}) = \rho_b(\vec{r}) / \int \rho_b(\vec{r}) d\vec{r} \quad (4)$$

#### 4.4.2 Several considerations

Several considerations follow although they do not yet provide quantitative conclusions.

- In general the suppression of  $\delta\rho$  loosens the condition for  $\delta A^{sp}$ , namely

$$|\delta P_T^{sp}| < |\delta\tilde{\rho}(\vec{r})|_{max} \cdot V \cdot \frac{|\delta A^{sp}(\vec{r})|_{max}}{\langle \alpha(\vec{r}) \rangle}. \quad (5)$$

If we can suppress  $|\delta\tilde{\rho}(\vec{r})|_{max} \cdot V$  to the level of  $10^{-3}$ ,  $|\delta A^{sp}(\vec{r})|_{max} < 3 \times 10^{-2}$  is enough to obtain  $|\delta P_T^{sp}| < 10^{-4}$ , assuming  $\langle \alpha(\vec{r}) \rangle \sim 0.3$ . This discussion is valid *vice versa*.

- Since  $\langle \delta\tilde{\rho}(\vec{r}) \rangle = 0$  and  $\delta\tilde{\rho}(\vec{r})$  should be a smooth function over the polarimeter volume, these conditions might loosen the constraints on  $|\delta A^{sp}(\vec{r})|_{max}$ . Furthermore, if the  $K_{\mu 3}$  kinematics is perfect the distribution  $\delta\rho(\vec{y})$  is symmetric about  $y = 0$  and nearly equal for  *fwd*  and  *bwd* . This condition might be helpful, too.
- If the  $K_{\mu 3}$  phase space is distorted due to the CsI(Tl) calorimeter misalignment or inefficiency distribution, or the incomplete tracking performance, the primary effect is the shift of the decay plane distribution which admixes  $P_N$  and  $P_L$  into  $P_T$ . This effect has to be removed in the decay plane analysis. The secondary effect is the distortion of  $\delta\rho(\vec{r})$  and the distribution is not necessarily symmetric about  $y = 0$ . It might be that  $|\delta A^{sp}(\vec{r})|_{max}$  should be limited even more.

#### 4.4.3 Monte Carlo studies

In order to determine the general behaviour of the asymmetry fluctuation in the presence of a wire displacement, a Monte Carlo simulation was performed. We assumed random displacements for the wire coordinates  $(x, y, z)$  for each wire, where  $y$  and  $z$  are the position of the wire and  $r(x)$  is the coordinate measured with sense wire charge division in which the position calibration might have a certain shift. Exaggerated displacements with a standard deviation ( $\sigma$ ) of 1mm in a Gaussian distribution function were assumed while the manufacturing tolerance is specified to be  $50\mu\text{m}$ . The calibration uncertainty in charge division is not well known yet but we assumed the same size of displacement with  $\sigma = 1$  mm. (The position resolution was taken into account.)

The realistic displacements might not be completely random but may have some locally collective displacement in a cluster. However, the random fluctuation should have such a situation with a certain probability. Namely a MC calculation for one set of displacements of all the wires may provide statistically meaningful data. The method here is the observation of the behavior of the asymmetry function to obtain an idea about the potentially maximum local spurious asymmetry and the fluctuation structure such as the average period in order to study the integrating-out characteristics of Eq.(1).

For tracking and detecting positrons, a realistic condition in the data analysis was employed. Tracking was performed using the first four chamber layers which was known to be optimal from the earlier MC studies. The high energy part of the spectrum ( $E > 35$  MeV) was selected and the cone angle was set to  $67^\circ$ . The asymmetry was calculated for all the gaps by stopping muons in the plates with  $z = -14$  to  $\sim 14$  cm. Fig.8 shows the asymmetry function obtained. As expected the variation structure is very irregular but the maximum value is less than about  $10^{-2}$  under the given input conditions.

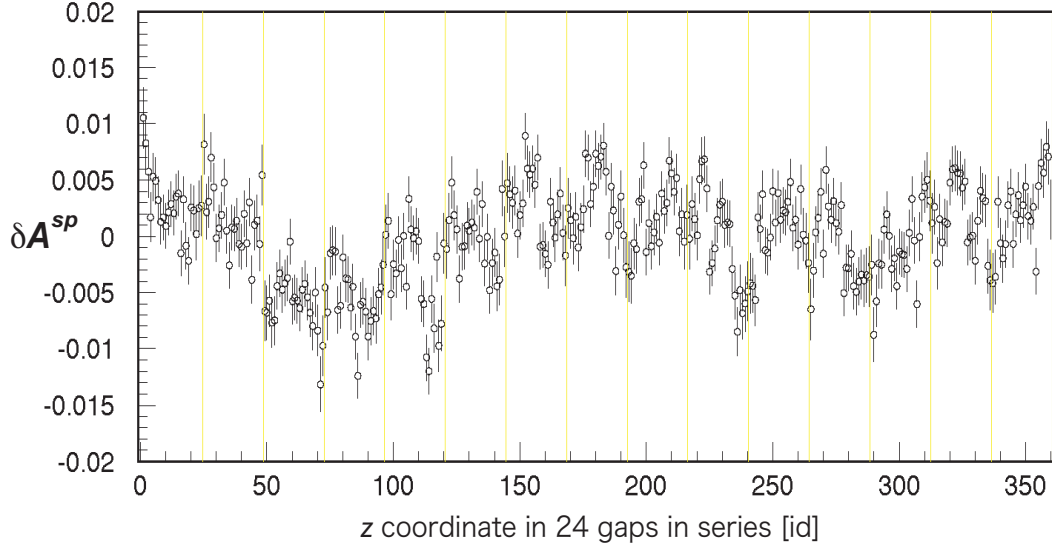


Figure 8: Local spurious asymmetry due to random wire displacement calculated in a MC simulation. The horizontal axis is the  $z$  coordinate of the muon stopping point in all the 24 gaps in series. Regarding the MC calculation input, see the text

#### 4.4.4 Discussions

The oscillation pattern depends of course on the input random displacement of the wires and Fig.8 is just one example. However, the existence of a number of structures allows us to do some discussions with a certain statistical meaning. We want to know how the integration of Eq.(1) cancels out “typically” the local spurious asymmetry effect. We know that the muon stopping distributions for “fwd” and “bwd” can be different mainly in the  $z$  and  $r$  directions due to the slightly different decay kinematics momentum range. In a simple model we assumed a Gaussian shape of the distribution for  $z$  and shifted the center by  $\pm 0.5$  cm as shown in Fig.9 (left) producing the normalized density difference function  $\delta\tilde{\rho}(\vec{r})$  in Eq.(1) of  $-0.012$  to  $+0.012$ . The  $r$  dependence is not relevant now since the random wire shift in the  $r$  direction is  $r$  independent. Also the  $y$  (gap) distribution is rather flat and left-right equal in the first order. Fig.9 (right) shows the results of a T-violating spurious asymmetry,  $A_T^{sp} = (A_{fwd} - A_{bwd})/2$ , after  $z$  integration plotted for each gap together with the original  $A_{fwd}$  and  $A_{bwd}$ . We see that the average asymmetry,  $A_T$ , is vanishingly small (it is less than  $10^{-4}$  for the total average of black point) leading to a sufficiently small  $\delta P_T^{sp}$  of less than  $1.5 \times 10^{-4}$ . If we stick to a more conservative assumption and take  $|\delta A^{sp}|_{max} < 1.5 \times 10^{-2}$  from Fig.7 to apply for Eq.(5), we obtain a constraint of  $|\delta\tilde{\rho}_{max}| \cdot V < 2 \times 10^{-3}$  to achieve  $|\delta P_T| < 10^{-4}$ .

However, we may regard that these constraints are scaling to the standard deviation of the assumed wire displacement distribution, which was exaggerated in the present simulation calculation. The realistic alignment precision of wires (in the  $z$ - $y$  plane) of  $50 \mu\text{m}$  and an accurate  $r$  calibration should reduce this spurious polarization drastically to a level much

less than  $10^{-4}$ . Of course we will perform an analysis to suppress the  $\delta\tilde{\rho}(\vec{r})$  distribution as much as possible. If necessary, we can symmetrize  $\rho_f(\vec{r})$  and  $\rho_b(\vec{r})$  at the cost of a small fraction of good events when the local spurious asymmetry is hard to eliminate.

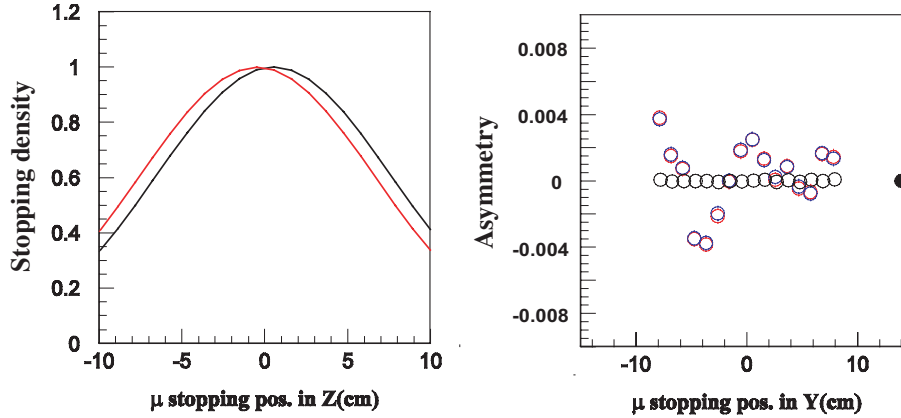


Figure 9: Left: Muon stopping distribution for pion *fwd* (black) and *bwd* (red) assumed in the MC simulation. Right: Average asymmetry for each layer; the asymmetry for *fwd* (blue), *bwd* (red), and the T-violating asymmetry  $A_T = (A_{fwd} - A_{bwd})/2$ . The black point is the total average of all the layers, which is  $(-0.18 \pm 0.78) \times 10^{-4}$ .

#### 4.5 Effects of non-uniform chamber inefficiency

The chamber inefficiency might not be uniform in a cell depending on the charged particle penetration point and also among cells depending on the wire and readout electronics conditions. The former phenomena might be significant in a cell with a large aspect ratio. One of the reasons why we want to test the prototype model is to investigate the inefficiency distribution. The inefficiency for a certain track or for a certain wire is, however, regarded not to cause a significant spurious asymmetry, since the left/right symmetry holds, namely the part of low efficiency is serving for both left going positions and right going positrons in the same manner.

In order to observe the general behaviour of the local spurious asymmetry, if any, even with a small size, we performed a simulation using a simple model. Only the wire efficiency was changed without any variation in the cell depending on the track position. The wire inefficiency was randomly given as in the case of the misalignment study. The efficiency distribution was assumed to have an average value of 99.5% and a width of  $\sigma_{ef} = 0.5\%$ . The standard  $e^+$  tracking method was employed and the asymmetry was calculated as a function of the gap and the  $z$ -coordinate. Fig.10 shows the behaviour of the asymmetry fluctuation. A very similar pattern was obtained as for the asymmetry due to the wire misalignments. The exactly same discussion as in the wire misalignment holds. A simulation with the same *fwd* and *bwd* distribution  $z$  direction shifts results in the total average asymmetry of  $A^{sp} = (-0.24 \pm 0.82) \times 10^{-4}$  corresponding to  $\delta P_T = (-0.8 \pm 2.7) \times 10^{-4}$ . We see here the necessity to suppress  $\delta\tilde{\rho}$  to less than the MC assumption.

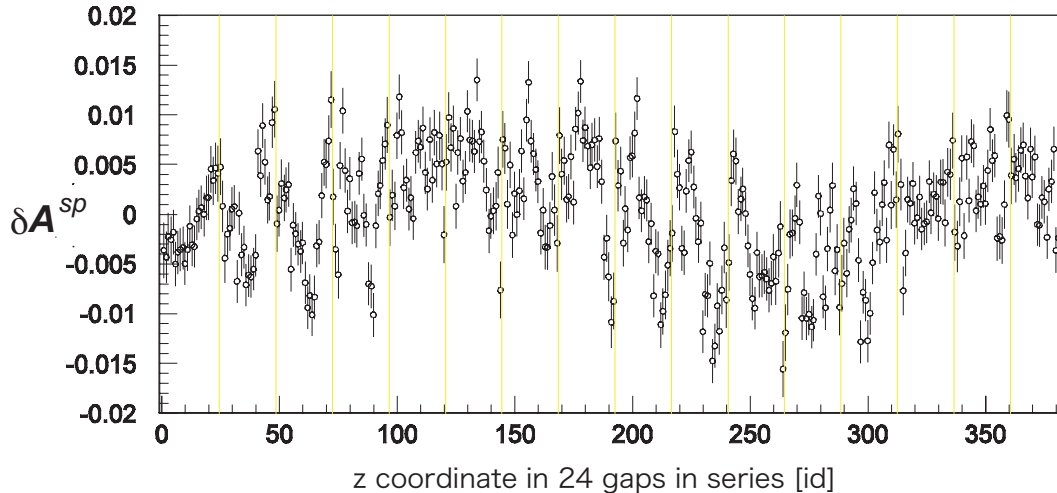


Figure 10: Local spurious asymmetry due to random chamber inefficiency distribution calculated in a MC simulation. The horizontal axis is the  $z$  coordinate of the muon stopping point in all the 24 gaps in series. Regarding the MC calculation input, see the text

More detailed studies will be performed using the inefficiency distribution data acquired in the prototype chamber test.

## 5 Summary

While continuing our every effort to secure total funding of the TREK experiment, we are proceeding with the detector element construction using our smaller budgets. The R&D, design and construction of the polarimeter and the target are going well. For the other detector elements the responsible teams are starting preparations. We are now further convinced of the overall validity of the TREK high precision muon polarization experiment. None of the Monte Carlo simulations, which we have performed up to now, have revealed any serious sources of systematic errors. We have shown that both global misalignments as well as any conceivable local effects in the polarimeter are controllable or insignificant, and such effects are considered to be the most dangerous systematics in the TREK experiment. We would like to be ready with the detector final design as we concentrate on the funding of the full experiment.

## References

- [1] J. Imazato *et al.*, “Measurement of  $\mu^+$  Relaxation Rate in Al and Mg Alloys for the Precise  $\mu^+$  Transverse Polarization Experiment TREK at J-PARC”, to appear in the Proceedings of the 11th International Conference on Muon Spin Rotation, Relaxation and Resonance, July 2008, Tsukuba, Japan.
- [2] F. Simon *et al.*, arXiv:0808.3477v1, accepted by Nucl. Instr. Meth., in press